Electronic and Geometrical Structure of the Sc[BO]$^+$ Cation. An Ab Initio Investigation

Aristotle Papakondylis and Aristides Mavridis*

Laboratory of Physical Chemistry, Department of Chemistry, National and Kapodistrian University of Athens, P.O. Box 64 004, 157 10 Zografou, Athens, Greece

Received: July 26, 1999; In Final Form: September 21, 1999

The Sc[BO]$^+$ molecular cation has been investigated theoretically by multireference CI methods. We have examined the potential energy surfaces of all states that correlate to the ground-state Sc$^+$(^{3}D) + BO($X^2\Sigma^+$) fragments. Three kinds of minima were discovered corresponding to the linear Sc−BO$^+$ and BOSc$^+$ and to the bent BOSc$^+$ configurations, with the bent structure being the global minimum for all states. Full potential energy curves are reported for all symmetries examined, i.e., ^{2}A′(3), ^{2}A″(2) for the bent and $^2\Delta$, $^2\Pi$, $^2\Sigma^+$, $^4\Delta$, $^4\Pi$, and $^4\Sigma^+$ for the linear geometries. The ground state is of ^{2}A″ symmetry with a BO−Sc binding energy D_e = 63.9 kcal/mol at an equilibrium geometry with B−OSc and BO−Sc bond lengths of 1.260 and 2.046 Å, respectively, and a BOSc angle of 90.7°.

1. Introduction

The chemistry of boron−oxygen compounds is characterized by an extraordinary complexity[1] and diversity. The simplest of them is BO, the exclusive product of boron atoms with O_2 in the gas phase,[2] a process that is highly exothermic making boron a potential high-energy fuel.

The principal oxide of boron is boric oxide (B_2O_3), which melts at 450°; above 450 °C polar BO groups are formed while fused B_2O_3 readily dissolves many metal oxides to give characteristically colored borate glasses.[1] The BO species appears to be an important intermediate in the oxidation process of boron and polymerizes to form a variety of boron−oxygen systems.

The ground state, $X^2\Sigma^+$ ($=1\sigma^2 2\sigma^2 3\sigma^2 4\sigma^2 5\sigma^1 \pi_x^2\, \pi_y^2$), of BO[3] can be characterized as a σ radical faithfully represented by the following valence bond Lewis (vbL) icon:

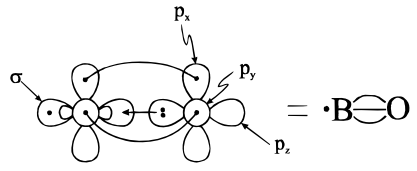

(1)

suggesting the formation of a triple bond between the B and O atoms. Note that the in situ B atom finds itself in the excited ^{4}P(M=0) state, 3.57 eV above its ground ^{2}P state.[4] The experimental binding energy (D_e) of BO is $D_e = D_0 + \omega_e/2$ = 8.40 eV,[3] or with an intrinsic bond strength (i.e, with respect to the diabatic fragments B(^{4}P) + O(^{3}P)) of 8.40 + 3.57 = 11.97 eV, much in line with the similarly bonded C≡O($X^1\Sigma^+$) system with D_e = 11.36 eV.[3]

Now the first excited state of BO is of $A^2\Pi$ symmetry ($=1\sigma^2 2\sigma^2 3\sigma^2 4\sigma^2 5\sigma^2 \pi^3$) 2.96 eV above the $X^2\Sigma^+$ ground state[3] and can be characterized as π radical with the single electron localized on the oxygen atom (icon 2).

The icons 1 and 2 of the $X^2\Sigma^+$ and $A^2\Pi$ BO states imply that the boron oxide (BO) can interact easily with a multitude of radicals R═H, F, Cl, Br, CH_3, ... to produce linear and bent

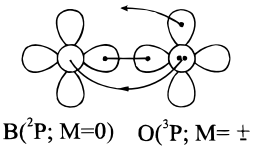

(2)

oxoborons of the type R−BO or BO−R, and indeed, this is the case.[5] Recently, Schaefer et al.,[6] examined the HBO and BOH systems at the CCSD(T)/TZ2P level of theory while Boldyrev and Simons[7] investigated the cations HBO^+ and BOH^+ at the QCISD(T)/6-311++G(2df, 2pd) level. It was found that while HBO is more stable than the two isomers, the BOH^+ isomer is more stable than HBO^+. Ab initio calculations of MP4/DZP// MP2/DZP type have been performed in the series R[BO], R═ H, F, Cl, CH_3[5] indicating that the R−BO species are more stable than BO−R bent isomers. The lithiated species LiBO and BOLi have been examined theoretically by Nemukhin et al.[8] and reexamined very recently together with X[BO], X = Na and K by Fuentealba[9] using DFT and G2 methods.

The present paper examines by ab initio techniques the transition metal molecular cation Sc[BO]$^+$ (Sc−BO$^+$ or BO−Sc$^+$). To the best of our knowledge, this is the first time that the interaction of the BO molecule with a transition metal is investigated theoretically. In particular, we study the potential energy surfaces of the species Sc−BO$^+$ and BO−Sc$^+$ correlating to the ground-state fragments Sc$^+$($4s^1 3d^1$;^{3}D) and BO($X^2\Sigma^+$) using multireference techniques. Because of the very unusual properties of boron oxides, we believe that the study of the Sc-[BO] $^+$ species can be used as a model system to facilitate the investigation of more complex boron oxide−metal systems by both experimentalists and theoreticians, and materials scientists in general.

2. Computational Approach

For the B and O atoms we employed the correlation consistent triple-ζ quality basis set, cc-pVTZ, of Dunning,[10] while for the metal atom the ANO basis of Bauschlicher[11] was used but with the functions of g symmetry removed. Our generalized contracted function space, [$(4s3p2d1f)_{B,O}$/$(7s6p4d3f)_{Sc}$], consists of 126 spherical Gaussians (5d and 7f functions).

10.1021/jp992585t CCC: $18.00
Published on Web 10/30/1999

In a complete valence CASSCF (complete active space SCF) calculation, the 11 valence (active) electrons ($[2s^2 2p^1]_B$, $[2s^2 2p^4]_O$, $[4s^1 3d^1]_{Sc}$) should be allowed to occupy a 14 active orbital molecular space, considering that the Sc^+ valence space consists of 6 orbitals (1s + 5d). Such an approach produces under $^2A'$ symmetry 1 289 178 configuration functions (CF), rendering even the CASSCF computations impractical. Instead, a CASSCF wave function was constructed by distributing three electrons (the two valence electrons on Sc^+ plus the single BO electron) among seven orbitals. This seven-orbital space ensures correct axial symmetry for the linear geometries ($|\Lambda|$ angular momentum) and correct asymptotic behavior of the Sc^+ + BO fragments. To treat equivalently linear and bent geometries, all calculations were done under C_s symmetry restrictions. The CASSCF space was state-averaged with equal weights over five states, namely, 3A′ + 2A″ corresponding to $\Delta^{\pm}$, $\Pi^{\pm}$, and Σ^+ symmetries of the linear geometries and consisting of 60A′ + 52A″ CFs for the doublets and 15A′ + 20A″ CFs for the quartets.

Valence "dynamical" correlation was obtained by single and double excitations of the 11 active electrons out of the previously described reference CAS space (CASSCF+1+2=MRCI). To keep our MRCI expansions manageable, the internally contracted MRCI (icMRCI) approach was followed,[12] thus reducing the uncontracted MRCI spaces by about a factor of 10. For instance, the 9 196 852 CFs MRCI space of the $^2\Delta(A')$ state of $Sc-BO^+$ is reduced to 713 088 CFs by internal contraction, a severe reduction of the functional space. However, our experience is, at least with the series of diatomics ScB^+, TiB^+, VB^+, and CrB^+,[13] that the icMRCI method, on the average, does not cause absolute energy losses larger than 2 mhartree; therefore, we believe that the quality of our MRCI wave functions remains practically unaffected because of the internal contraction approach. Geometry optimizations were carried out at the MRCI level using either numerical gradients or energy grids for certain partial optimizations. Finally, all MRCI calculations are size extensive within 1 mhartree with respect to the CISD (SCF +1+2) fragments.

For all computations the MOLPRO96[14] package was employed.

3. Fragments Sc^+ and BO

The SCF and CISD (SCF+1+2) energies of the ground state $^3D(4s^1 3d^1)$ of Sc^+ are −759.540 45 and −759.545 13 hartree, respectively. The corresponding numerical Hartree−Fock value is −759.539 144 hartree,[15] 1.3 mhartree *higher* than our value because of C_{2v} symmetry restrictions imposed on the SCF calculation. At the CISD level energy splittings $\Delta E(^3F \leftarrow ^3D) = 0.703$ and $\Delta E(^1D \leftarrow ^3D) = 0.272$ eV are obtained, compared to the experimental values of 0.596 and 0.302 eV,[4] respectively.

Table 1 lists calculated properties of the ground $X^2\Sigma^+$ and $A^2\Pi$ state of BO at the CISD level along with available experimental results. While the agreement between experimental and theoretical bond distances for both states can be considered as good, the same cannot be said for the D_e value of the $X^2\Sigma^+$ state. The 22.5(15) kcal/mol difference between the experimental and CISD (CISD+Q) values is due to the medium size basis set used but primarily to the size nonextensivity error introduced by the CISD tecnique. Observe the polarity flip between the $X^2\Sigma^+$ and $A^2\Pi$ states, as is evidenced by the algebraic values of the dipole moment of these two states. Finally, the atomic CISD Mulliken populations of the $X^2\Sigma^+$ and $A^2\Pi$ states,

TABLE 1: SCF and CISD Energies *E* (hartree), Bond Distances R_e (Å), Dissociation Energies D_e (kcal/mol), Dipole Moments μ (D), and Energy Separation T_e (eV) of the $X^2\Sigma^+$ and $A^2\Pi$ States of BO

method	*E*	R_e	D_e	μ^d	T_e
		$X^2\Sigma^+$			
SCF	−99.55398	1.180	138.2	−2.83	0.0
CISD[a]	−99.83792	1.200	171.2	−2.37	0.0
CISD+Q[b]	−99.8622	1.209	178.9		0.0
exptl[c]		1.2045	192.8		0.0
		$A^2\Pi$			
SCF	−99.47586	1.338		+1.01	2.13
CISD[a]	−99.73846	1.354		+1.03	2.71
CISD+Q[b]	−99.7623	1.362			2.72
exptl[c]	-	1.3533			2.96

[a] SCF + single + double replacements. [b] Davidson's corrections for quadruple replacements. [c] Reference 3. [d] The minus sign corresponds to a $^{\delta+}B-O^{\delta-}$ polarity.

$$X^2\Sigma^+:\ 2s^{1.05}2p_x^{0.41}2p_y^{0.41}2p_z^{0.73}(d+f)^{0.16}/\\ 2s^{1.69}2p_x^{1.52}2p_y^{1.52}2p_z^{1.49}(d+f)^{0.03}$$

and

$$A^2\Pi:\ 2s^{1.82}2p_x^{0.09}2p_y^{0.22}2p_z^{0.74}(d+f)^{0.15}/\\ 2s^{1.78}2p_x^{0.91}2p_y^{1.72}2p_z^{1.54}(d+f)^{0.04}$$

for B and O, respectively, confirm our previously given vbL icons 1 and 2. Note that in the $X^2\Sigma^+$ state, ∼1.1 e^- are transferred from B to O via the π frame with a synchronous migration of about 0.8 e^- from O to B via the σ frame, resulting in a net transfer of about 0.25 e^- from B to O. In the $A^2\Pi$ state the 2s bonding participation for both atoms can be practically ignored, while the symmetry-carrying electron is essentially localized on a $2p_x$(O) orbital with the O atom barely positively charged.

Inasmuch as our purpose is not an accurate description of the BO molecule but its bonding interaction with Sc^+, the CISD description of BO to which our MRCI $ScBO^+$ wave function corelates is clearly adequate.

4. Results and Discussion

4.1. Doublets. The approach of $Sc^+(^3D)$ to either side of the $BO(X^2\Sigma^+)$ molecule can give rise to doublet and quartet potential energy surfaces. Figure 1 shows the doublet minimum energy profiles of the $Sc^+(^3D)\cdots BO(X^2\Sigma^+)$ interaction, parametrized with respect to the angle $\theta = \angle B-O-Sc$ (see inset, Figure 1). These profiles are constructed by optimizing the B−O and B−Sc or O−Sc distances using energy grids for a series of fixed θ values; linear geometries of $Sc-BO^+$ and $BO-Sc^+$ correspond to $\theta = 0.0°$ and $\theta = 180.0°$, respectively. The lifting of the ^3D Sc^+ degeneracy due to axial BO interaction gives rise to the $^2\Sigma^+$, $^2\Pi^{\pm}$, and $^2\Delta^{\pm}$ Sc[BO]$^+$ states. By bending the molecule ($\theta \neq 0.0°$ or 180.0°), the $\Pi^{\pm}$ and $\Delta^{\pm}$ degeneracies are further lifted, resulting in a total of five states $^2A'(3)$ and $^2A''(2)$ (Figure 1).

As can be seen from the curves shown in Figure 1, three different minima were found for each state examined: two (local) corresponding to the linear isomers $Sc-BO^+$ or $BO-Sc^+$ ($^2\Delta$, $^2\Pi$, $^2\Sigma^+$), and one global minimum that corresponds to the bent structure ($^2A'$, $^2A''$) for all states, with θ between 80 and 90°. To confirm the existence of these minima, we performed complete geometry optimizations using numerical gradients, which indeed gave the same results as the point-by-

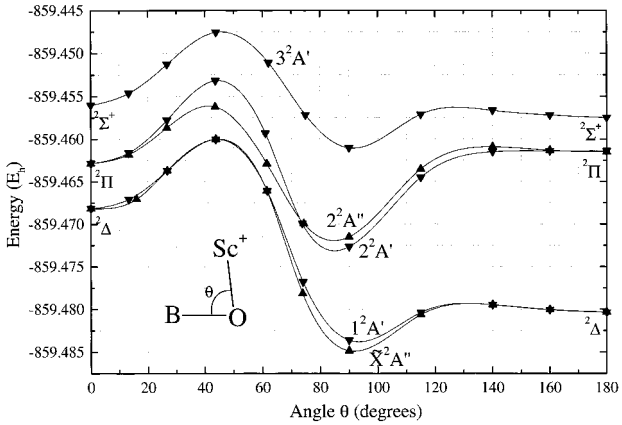

Figure 1. Energy profiles with respect to the angle $\theta = \angle$BOSc of the Sc[BO]$^+$ at the MRCI level of theory.

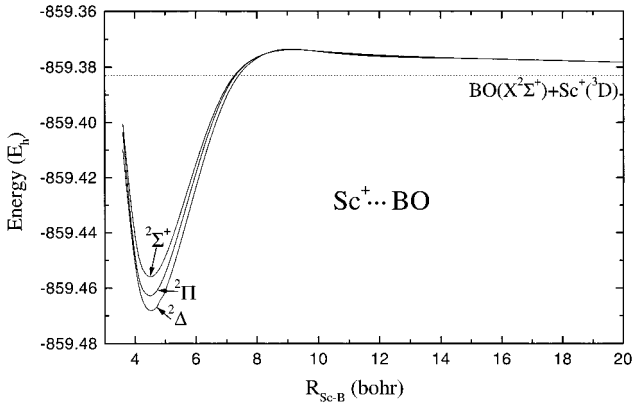

Figure 2. MRCI potential energy curves of the linear Sc−BO$^+$ $^2\Delta$, $^2\Pi$, and $^2\Sigma^+$ states as a function of the Sc−B distance. The dotted line corresponds to the asymptotic energy of the ground-state fragments.

point optimizations. Nevertheless, the BO−Sc$^+$ linear structures can only technically be characterized as minima, being separated from their global minima by energy barriers of about 1 mhartree (Figure 1).

4.1.a. Sc−BO$^+$ Linear Geometry. The approach of the Sc$^+$(^{3}D, 3d^{1}4s^1) cation from the B side of the BO molecule is expected to interact attractively by forming a σ type bond, giving rise to three molecular states of $^2\Sigma^+$, $^2\Pi$, or $^2\Delta$ symmetry, depending on the symmetry-carrying Sc$^+$ electron σ, π, or δ, respectively. This is illustrated by the following:

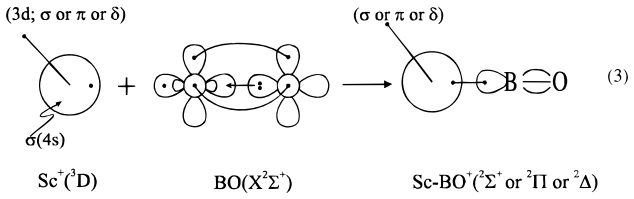

(3)

The above picture is confirmed by our calculations. Table 2 presents total energies, geometries, Sc−BO$^+$ dissociation energies, and Mulliken charges at the MRCI level of theory, and Figure 2 shows potential energy curves (PEC) of the $^2\Delta$,$^2\Pi$, and $^2\Sigma^+$ states. We see that the ground state of the linear Sc−BO$^+$ geometry is of $^2\Delta$ symmetry with the $^2\Pi$ and $^2\Sigma^+$ states lying 3.50 and 8.80 kcal/mol above the $^2\Delta$ state. The ordering of the states is more or less expected, considering the diminishing repulsive interaction of the σ, π, or δ observer Sc$^+$ electron with the BO σ or π electron distribution. Upon binding with Sc$^+$, the B−O bond is practically not perturbed at all (cf. Tables 1 and 2) while the symmetry-carrying electron is completely localized in the corresponding orbital of the Sc$^+$ ion with no participation in the chemical bonding. Also, about 0.1 e$^-$ is transferred from Sc$^+$ to the BO system. Although the $^2\Delta$, $^2\Pi$, and $^2\Sigma^+$ PECs are exactly size extensive with respect to Sc$^+$(^{3}D)+BO($^2\Sigma^+$) CISD fragments, this is not obvious from Figure 2; the long-range repulsive part of the PECs with a 2.3 kcal/mol maximum at about 9.0 bohr mirrors the electrostatic repulsion between Sc$^+$ and the positive end of the incoming B−O dipole.

Finally, Sc$^+$−BO binding energies are D_e = 53.4, 49.9, and 44.6 kcal/mol for $^2\Delta$,$^2\Pi$, and $^2\Sigma^+$ states, respectively, at the MRCI level of theory. A uniform increase of D_e's by about 4 kcal/mol is obtained when the multireference Davidson's correction is taken into account.

4.1.b. Sc[BO]$^+$ Bent Geometry. By bending the (linear) Sc−BO$^+$ species, five states of symmetries ^{2}A′(3) and ^{2}A″(2) are obtained (Figure 1). For all states we have to surmount an energy barrier ranging from 4 to 6 kcal/mol, which is due to the breaking of the σ Sc−B bond with the synchronous formation of a σ Sc−O bond (but see below), resulting in a ground state of $\tilde{X}^2$A″ symmetry adiabatically correlating to the $^2\Delta$ state. From Figure 1 we observe that for all potential energy surfaces, global

TABLE 2: Total Energies *E* (hartree), Bond Distances *R* (Å), Angles θ (deg), Dissociation Energies D_e and D_e(+Q) (kcal/mol), and Mulliken Charges *q* of the Linear Sc−BO$^+$ and BO−Sc$^+$ and Bent Sc[BO]$^+$ Isomers at the MRCI Level of Theory

state	$-E$	R_{B-O}	R_{B-Sc}	R_{O-Sc}	q	D_e	D_e(+Q)[a]	q_B	q_O	q_{Sc}
					Sc−BO$^+$					
$^2\Delta$	859.468 14	1.202	2.402		0.0	53.4	57.3	−0.04	−0.08	+1.12
$^2\Pi$	859.462 56	1.202	2.378		0.0	49.9	54.0	−0.02	−0.09	+1.11
$^2\Sigma^+$	859.454 12	1.200	2.385		0.0	44.6	49.4	−0.03	−0.08	+1.11
					Sc[BO]$^+$					
$\tilde{X}^2$A″	859.484 85	1.260	2.416	2.046	90.7	63.9	65.9	0.00	−0.24	+1.24
1^2A′	859.483 60	1.259	2.440	2.044	92.1	63.1	65.1	0.00	−0.25	+1.25
2^2A′	859.473 10	1.255	2.350	2.105	84.7	56.5	59.2	+0.01	−0.24	+1.23
2^2A″	859.472 07	1.246	2.380	2.151	84.5	55.9	58.1	+0.01	−0.23	+1.22
3^2A′	859.461 04	1.256	2.438	2.093	89.8	48.9	52.1	−0.01	−0.24	+1.25
					BO−Sc$^+$					
$^2\Delta$	859.480 31	1.302		1.919	180.0	61.0	62.0	−0.10	−0.40	+1.50
$^2\Pi$	859.461 45	1.294		1.955	180.0	49.2	50.6	−0.12	−0.39	+1.51
$^2\Sigma^+$	859.457 45	1.313		1.893	180.0	46.7	49.3	−0.07	−0.39	+1.46
$^4\Delta$	859.434 10	1.213		2.228	180.0	32.0	31.3	+0.37	−0.24	+0.87
$^4\Pi$	859.428 07	1.212		2.257	180.0	28.3	27.6	+0.36	−0.23	+0.87
$^4\Sigma^+$	859.413 72	1.211		2.453	180.0	19.3	18.6	+0.35	−0.24	+0.89

[a] With Davidson's multireference correction.

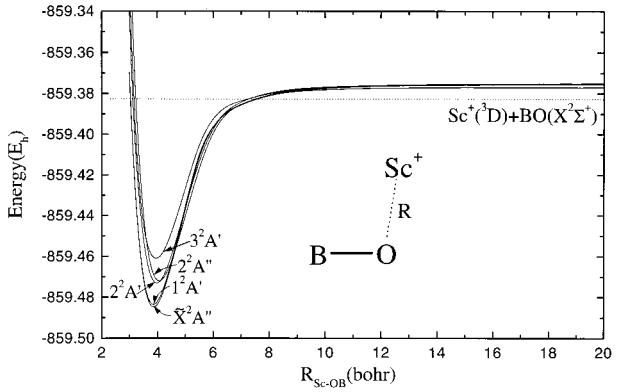

Figure 3. MRCI potential energy curves of the $BOSc^+$ states ($\tilde{X}^2A''$, $1^2A'$, $2^2A'$, $2^2A''$, $3^2A'$) as a function of the O−Sc separation. For all states the B−O distance and the BOSc angle were kept at their equilibrium values.

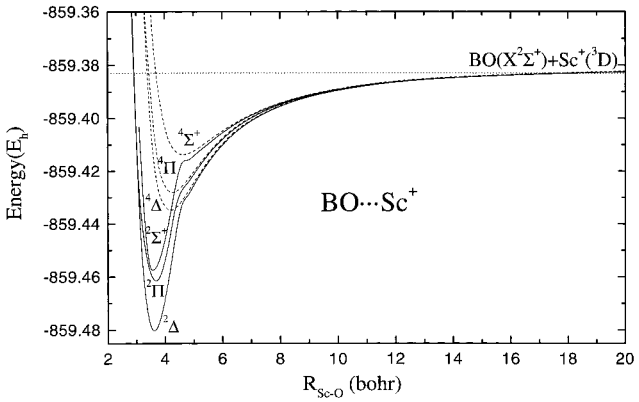

Figure 4. MRCI potential energy curves of the linear BO−Sc^+ doublet and quartet states ($^2\Delta$, $^2\Pi$, $^2\Sigma^+$, $^4\Delta$, $^4\Pi$, $^4\Sigma^+$) as a function of the O−Sc distance. The B−O distance is optimized at every calculated point.

minima are of either $^2A'$ or $^2A''$ symmetry at an angle of about 90° (Table 2).

The equilibrium Mulliken MRCI atomic populations of the $\tilde{X}^2A''$ ground state are

$$4s^{0.24}3d_{z^2}{}^{0.06}3d_{x^2-y^2}{}^{0.10}3d_{xy}{}^{0.07}3d_{xz}{}^{0.08}3d_{yz}{}^{1.00}3p^{0.13}/Sc$$

$$2s^{1.44}2p_x{}^{0.39}2p_y{}^{0.29}2p_z{}^{0.80}3d^{0.16}/B$$

and

$$2s^{1.70}2p_x{}^{1.51}2p_y{}^{1.55}2p_z{}^{1.44}3d^{0.05}/O$$

The populations of the rest of the states are practically identical with the above distributions, the only exception being the observer, symmetry-carrying electron, which is distributed to the Sc^+ atomic orbitals as $3d_{z^2}{}^{0.69}3d_{x^2-y^2}{}^{0.44}$, $3d_{xz}{}^{0.97}$, $3d_{yz}{}^{0.97}$, and $3d_{z^2}{}^{0.40}3d_{x^2-y^2}{}^{0.60}$ for $1^2A'$, $2^2A'$, $2^2A''$, and $3^2A'$, respectively. In all states 0.20−0.25 e^- are transferred from the metal atom to the −BO moiety. From Table 2 we can see that although formally the ground state is of $^2A''$ symmetry, the $\tilde{X}^2A''$ and $1^2A'$ can be considered as degenerate within the accuracy of our calculations, their energy difference being 0.78 kcal/mol. The same can be said for the next pair of states ($2^2A'$, $2^2A''$), which differs by only 0.65 kcal/mol. Figure 3 shows PECs for all five states at the MRCI level, constructed by keeping the B−O distance and the BOSc angle at the corresponding equilibrium values and varying the O−Sc distance. All PECs correlate to $Sc^+(^3D)$ + $BO(X^2\Sigma^+)$, and by allowance for the relaxation of the BO system, our MRCI calculations are size extensive. Binding energies range from 48.9 ($3^2A'$) to 63.9 kcal/mol ($\tilde{X}^2A''$) (Table 2). A natural question that is raised at this point is how the bonding occurs in the bent states. We believe that the in situ BO moiety in the, for instance, $\tilde{X}^2A''$ state finds itself in at least a partially excited state or that in the bonding process the excited $^2\Pi$ state of BO (icon 2) has a strong participation. A vbL icon can be helpful in illustrating our ideas,

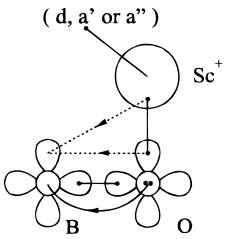

(4)

suggesting a three center−two electron bond between Sc^+ and BO. The above picture can be corroborated by observing that (a) in all five states the BOSc angle is very close to 90° (Table 2), (b) the B−O bond length ranges from 1.25 to 1.26 Å depending on the state, a value between the bond distance of the $X^2\Sigma^+$ and $^2\Pi$ states of the free BO molecule (Table 1), (c) the 2s atomic population on B and for all five bent states is ∼1.45 e^-, in contrast to 1.05 ($X^2\Sigma^+$) and 1.82 ($^2\Pi$) e^- for free BO (vide supra).

4.1.c. Sc−OB$^+$ Linear Geometry. The approach of the $Sc^+(^3D)$ to the oxygen site of the BO system in a linear fashion can give rise to doublets and quartets of Δ, Π, and Σ^+ symmetries in complete analogy with the $Sc^+\cdots BO$ linear attack (see section 4.1.a). Location of the $^2\Delta$, $^2\Pi$, and $^2\Sigma^+$ states with respect to the previously calculated linear and bent states is shown in Figure 1. While the $ScBO^+$ $^2\Delta \leftarrow {}^2\Pi$ and $^2\Sigma^+ \leftarrow {}^2\Pi$ splittings are almost equal, the corresponding energy separations of the Sc−BO^+ isomer differ significantly (Figure 1, Table 2), with the $^2\Delta$ Sc−OB^+ state being the lowest among all the linear states. From Table 2 we observe that the bond lengths increase by about 0.05 Å going from the linear Sc−BO^+ to the bent Sc$[BO]^+$ isomer and by an equal amount from the bent to the linear Sc−OB^+ structure. Binding energies of the $^2\Delta$, $^2\Pi$, and $^2\Sigma^+$ Sc−OB^+ states are 61.0, 49.2, and 46.7 kcal/mol, respectively, with respect to the ground-state fragments. Their potential energy curves at the MRCI level, obtained by optimizing the B−O distance for every calculated BO−Sc^+ point, are shown in Figure 4. It is interesting to report that as the $Sc^+(^3D)$ approaches the $BO(X^2\Sigma^+)$ system from infinity, the B−O distance remains practically the same and equal to ∼1.20 Å, up to about 4.7 b. At this point the B−O bond length increases abruptly to ∼1.28 Å with a concomitant change of the PECs' slope (Figure 4). At equilibrium the final B−O distance is about 1.30 Å for all three states (Table 2). This is an indication of the involvement of higher states of $^2\Sigma^+$, $^2\Pi$, and $^2\Delta$ symmetry, possibly stemming from a second $^2\Sigma^+$ state of BO ($B^2\Sigma^+$) lying 5.35 eV above the $X^2\Sigma^+$ and with a bond length of 1.305 Å.[3] It is also of interest to note that in every state, about 0.5 e^- are transferred from Sc^+ to the BO moiety despite the fact that the metal carries already a charge of +1. Although such a large electron transfer from Sc^+ to BO seems rather strange, it can be understood if we think of the very large Coulombic stabilization that is obtained as being due to such a transfer, ∼(+1.5)(−0.5)/4.0 au, or about −5 eV.

The atomic Mulliken equilibrium MRCI distributions, for instance, for the $^2\Delta$ state, are

$$4s^{0.08}3d_{z^2}{}^{0.13}3d_{x^2-y^2}{}^{1.00}3d_{xy}{}^{0.00}3d_{xz}{}^{0.09}3d_{yz}{}^{0.09}3p^{0.11}/Sc$$

$$2s^{1.79}2p_x{}^{0.20}2p_y{}^{0.18}2p_z{}^{0.79}3d^{0.14}/B$$

$$2s^{1.71}2p_x{}^{1.67}2p_y{}^{1.66}2p_z{}^{1.32}3d^{0.04}/O$$

The $^2\Pi$ and $^2\Sigma^+$ states have analogous distributions. The interesting point to note from the above populations is that the in situ 4s metal orbital loses almost 1 e$^-$ while the σ frame of the BO moiety hosts 1.79 + 0.79 + 1.32 = 3.90 e$^-$. The following vbL picture

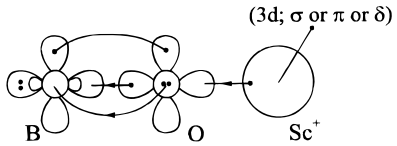

(5)

is in accord with the previous discussion.

4.2. Quartets. As was previously mentioned, the interaction of the Sc$^+$(^{3}D) + BO($X^2\Sigma^+$) molecular entities can also give rise to quartet states.

The investigation of the whole surface, in every symmetry, at the MRCI level proves that bound quartet states exist only for the linear BO···Sc$^+$ attack. Potential energy curves of $^4\Delta$, $^4\Pi$, and $^4\Sigma^+$ symmetries are shown in Figure 4. Corresponding binding energies are 32.0($^4\Delta$), 28.3($^4\Pi$), and 19.3($^4\Sigma^+$) kcal/mol at 2.23, 2.26, and 2.45 Å, respectively (Table 2).

Our MRCI equilibrium Mulliken populations, for instance, for the $^4\Delta$ state,

$$4s^{0.91}3d_{z^2}{}^{0.10}3d_{x^2-y^2}{}^{1.00}3d_{xy}{}^{0.00}3d_{xz}{}^{0.02}3d_{yz}{}^{0.02}3p^{0.11}/Sc$$

$$2s^{1.08}2p_x{}^{0.34}2p_y{}^{0.34}2p_z{}^{0.74}3d^{0.13}/B$$

$$2s^{1.68}2p_x{}^{1.57}2p_y{}^{1.57}2p_z{}^{1.37}3d^{0.04}/O$$

the relatively large bond distances, the weak interactions compared with those of the doublets, and the whole morphology of the PECs clearly suggest the electrostatic nature of the bonding with a synchronous transfer via the σ system of about 0.1 e$^-$ from BO to Sc$^+$. As expected, the in situ BO bond length is practically the same as that of the free BO($X^2\Sigma^+$). The whole situation is captured by the following vbL icon:

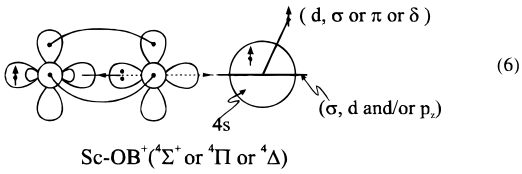

(6)

5. Summary

The electronic and geometrical structure of the molecular system Sc[BO]$^+$ has been investigated theoretically by CASSCF and MRCI methods using cc-pVTZ (B, O) and ANO (Sc) basis sets. Our main findings can be summarized as follows.

a. On the doublet potential surfaces, linear states Sc−BO$^+$ and BO−Sc$^+$ of $^2\Delta$, $^2\Pi$, and $^2\Sigma^+$ symmetries are local minima, with the lowest being BO−Sc$^+$ of $^2\Delta$ symmetry. The global minimum for all surfaces is of bent configuration with a ground state of $\tilde{X}^2A''$ symmetry, a binding energy D_e = 63.9 kcal/mol with respect to Sc$^+$(^{3}D) + BO($X^2\Sigma^+$) fragments, and a BOSc angle of 90.7°. A similarity of the Sc[BO]$^+$ to the R[BO] system, where R = Li, Na, K,[9] should be mentioned here. At the B3LYP and G2MP2 levels three minima were detected corresponding to the linear R−BO, BO−R, and the bent BOR configurations. The BOR angle ranges from 90° to 100° depending on the alkalimetal.

b. For all geometries and doublet states we have electron transfer from Sc$^+$ to BO, ranging from ∼0.1 e$^-$ (Sc−BO$^+$) to ∼0.5 e$^-$ (BO−Sc$^+$).

c. The in situ BO bond length compared to the free BO($X^2\Sigma^+$) remains the same in the Sc−BO$^+$ $^2\Delta$, $^2\Pi$, and $^2\Sigma^+$ states, while it is increased by about 0.05 and 0.1 Å in the bent and BO−Sc$^+$ linear geometries, respectively.

d. It seems that in the bent and BO−Sc$^+$ linear geometries, the $A^2\Pi$ and $B^2\Sigma^+$ states of BO are entailed in the bonding process.

e. Quartet minima were found only for the linear BO−Sc$^+$ geometry of Δ, Π, and Σ^+ spatial symmetries with binding energies of about half of the doublets. The binding mechanism of the quartets is mainly of electrostatic nature.

References and Notes

(1) Greenwood, N. N.; Earnshaw, A. *Chemistry of the Elements*; Pergamon Press: Oxford, 1990.
(2) Hanner, A. W.; Gole, J. L. *J. Chem. Phys.* **1980**, *73*, 5025.
(3) Huber, K. P.; Herzberg, G. *Molecular Spectra and Molecular Structure: IV. Constants of Diatomic Molecules*; Van Nostrand Reinhold Co.: New York, 1979.
(4) Moore, C. E. *Atomic Energy Levels*; NSRDS-NBS Circular No. 35; U.S. GPO: Washington, DC, 1971.
(5) Nguyen, M. T.; Groarke, P. J.; Ha, T.-K. *Mol. Phys.* **1992**, *75*, 1105 and references therein.
(6) Richards, C. A.; Vacek, G.; DeLeeuw, B. J.; Yamaguchi, Y.; Schaefer, H. F., III. *J. Chem. Phys.* **1995**, *102*, 1280.
(7) Boldyrev, A. I.; Simons, J. *J. Chem. Phys.* **1999**, *110*, 3765.
(8) (a) Nemukhin, A. V.; Almlöf, J. E.; Heiberg, A. *Theor. Chim. Acta* **1981**, *59*, 9. (b) Nemukhin, A. V.; Stepanov, N. F. *Theor. Chim. Acta* **1985**, *67*, 287.
(9) Fuentealba, P. *Chem. Phys. Lett.* **1999**, *301*, 59.
(10) Dunning, T. H., Jr. *J. Chem. Phys.* **1989**, *90*, 1007.
(11) Bauschlicher, C. W., Jr. *Theor. Chim. Acta* **1995**, *92*, 183.
(12) (a) Werner, H.-J.; Knowles, P. J. *J. Chem. Phys.* **1988**, *89*, 5803. (b) Knowles, P. J.; Werner, H.-J. *Chem. Phys. Lett.* **1988**, *145*, 514.
(13) (a) Kalemos, A.; Mavridis, A. *Adv. Quantum Chem.* **1998**, *32*, 69. (b) Kalemos, A.; Mavridis, A. *J. Phys. Chem. A* **1998**, *102*, 5982. (c) Kalemos, A.; Mavridis, A. *J. Phys. Chem. A* **1999**, *103*, 3336. (d) Kalemos, A.; Mavridis, A. Unpublished results of this laboratory.
(14) MOLPRO is a package of ab initio programs written by Werner, H.-J.; Knowles, P. J. with contributions from Almlof, J.; Amos, R. D.; Berning, A.; Deegan, M. J. O.; Eckert, F.; Elbert, S. T.; Hambel, C.; Lindh, R.; Meyer, W.; Nicklass, A.; Peterson, K.; Pitzer, R.; Stone, A. J.; Taylor, P. R.; Mura, M. E.; Pulay, P.; Schuetz, M.; Stoll, H.; Thorsteinsson, T.; Cooper, D. L.
(15) Hay, P. J. *J. Chem. Phys.* **1977**, *66*, 4377.